

79-1555

**Fully Conservative Numerical Solutions for
Unsteady Irrotational Transonic Flow
About Airfoils**

R. Chipman,
Grumman Aerospace Corp.,
Bethpage, N.Y.;;
and A. Jameson,
New York University,
New York, N.Y.

**AIAA 12th FLUID AND PLASMA
DYNAMICS CONFERENCE**

July 23 - 25, 1979/ Williamsburg, Virginia

For permission to copy or republish, contact the American Institute of Aeronautics and Astronautics-1290
Avenue of the Americas, New York, N.Y. 10019

UNSTEADY IRRATIONAL TRANSONIC FLOW ABOUT AIRFOILS

Richard Chipazan* and Antony Jameson**

SUMMARY

Numerical difference schemes are presented for the computation of unsteady transonic flows about airfoils. A first-order system of equations in conservation form is developed for irrotational (full potential) flow and solved by finite difference methods. To enable the boundary conditions to be imposed directly on the airfoil surface, a time-varying sheared-rectilinear coordinate transformation is used. Explicit differencing schemes are used to solve both lifting and non-lifting cases. Additionally, an alternating direction implicit (ADI) scheme has been coded for efficient solutions in the non-lifting case. Calculated time-accurate solutions for several cases are compared with the results of other unsteady transonic codes. Good correlation is shown with results produced by the more exact but computationally slower Euler-equations codes. Shock location is demonstrated to be better predicted than by small-perturbation or quasi-conservative schemes.

TABLE OF SYMBOLS

a	local speed of sound
c	chord length
D_x, D_y	central difference operators in X and Y directions
D_x^-, D_y^-	backward difference operators in X and Y directions
D_x^+, D_y^+	forward difference operators in X and Y directions
F	defined in Equation (9)
G	“ “ “
h	stagnation enthalpy
I	identity matrix
M	local Mach number
P	artificial viscosity terms
p	pressure
Q	velocity vector
S	defined In Equation (5)
t, T	time

TH	thickness ratio
U, v	velocity components
W	defined in Equation (9)
x, X	streamwise coordinate
y, Y	vertical coordinate
γ	specific heat ratio
ΔT	time step
ε	artificial viscosity constant
ρ	density
∞	Far-field condition, when used as subscript
λ	Courant number
τ	time in chord lengths traveled

INTRODUCTION

The transonic flow regime has long been known to be the most critical for flutter and other unsteady aeroelastic phenomena. Until recently, no efficient method has been available to calculate unsteady aerodynamics in this speed range; consequently, transonic flutter prediction has relied on wind tunnel testing. With the advent of faster computers and the emphasis on transonic cruise and maneuver capabilities for new aircraft design, much progress has been made recently in the development of both steady and unsteady transonic computational methods.

In unsteady transonic aerodynamics, work has proceeded along two different lines. In the first, researchers have produced linearized unsteady solutions about nonlinear mean (steady) flows. The efforts of Ehlers¹; Traci, Albano and Farr²; Cunninham³; Liu⁴; and rung, Yu and Seebass⁵ are examples of this approach. From experimental measurements such as those of Tijdeman⁶, it has been obvious that these linearized solutions are valid for a severely limited set of problems. Consequently, other researchers have pursued a second approach, the use of finite difference methods to obtain solutions to the coupled steady/unsteady flow. In this area, the works of Magnus and Yoshjara⁷; Lerat and Sides⁸; Beam and Warming⁹; Ballhaus and Steger¹⁰; Ballhaus and Goorjian¹¹⁻¹²; and Isogai¹³ are notable. The former three efforts have produced methods for solving the full Euler equations, which (although computationally too expensive for routine use) do provide excellent benchmark calculations. Ballhaus' works have produced an efficient method for solving the low-frequency, small perturbation form of the potential equation, thus making

* Senior Aeroelasticity Engineer, Structural Mechanics Section, Grumman Aerospace Corporation, Bethpage, New York. AIA.A Member.

** Professor, Computer Science, Courant Institute of Mathematical Sciences, New York University, New York, N. Y.

possible economic solutions to a range of important transonic unsteady problems.

Isogai developed the first solution procedure for the unsteady full-potential equations. The present effort improves on this procedure by constructing an algorithm for unsteady potential flow in true conservation-law form. Such a formulation enables realistic resolution of shock-wave locations necessary for accurate steady-state solutions. While this paper was in preparation, Goorjian¹⁴ also formulated a method for solving the unsteady potential equation in conservation form.

In the present paper, a system of equations for 2D, inviscid, irrotational, isentropic flow are written in conservation-law form using the primitive variables: density, streamwise velocity and stream-normal velocity. The equations are transformed to a time-varying, sheared-rectilinear-coordinate system with care taken to maintain the conservation form. Details of both explicit and implicit finite-difference schemes are presented for time-accurate solutions of the equations. Pilot computer codes have been written to implement the explicit scheme for both non-lifting and lifting cases and the implicit scheme for the non-lifting case only. Results of calculations from both codes for various sample problems are given and compared to published computations from other methods.

THEORY

For unsteady flow, the equations of mass and momentum conservation can be written

$$\frac{\partial \rho}{\partial t} + \bar{\nabla} (\rho \bar{Q}) = 0, \quad (1)$$

$$\frac{\partial \bar{Q}}{\partial t} + \bar{\nabla} \left(\frac{\bar{Q}}{2} \right) + \frac{1}{\rho} \bar{\nabla} \rho - \bar{Q}_x \bar{\nabla}_x \bar{Q} = 0 \quad (2)$$

For irrotational (potential) flow, the last term of the momentum equation is zero. If isentropic flow is assumed (which is a valid approximation when only weak shocks are present), this equation may be rewritten

$$\frac{\partial \rho}{\partial t} \begin{pmatrix} u \\ v \end{pmatrix} + \bar{\nabla} h = 0 \quad (3)$$

$$\text{Where } h = \frac{u^2 + v^2}{2} + \frac{\rho^{\lambda-1}}{(\lambda-1)M_\infty^2} - h_\infty$$

Thus, Equations C and (3) can be simply written in conservation form as -

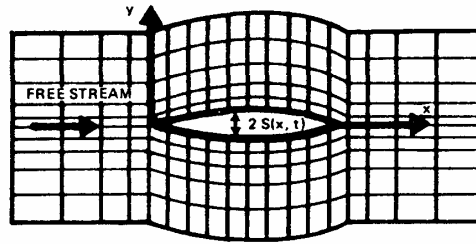
$$\frac{\partial}{\partial t} \begin{pmatrix} \rho \\ u \\ v \end{pmatrix} = \frac{\partial}{\partial x} \begin{pmatrix} \rho u \\ h \\ 0 \end{pmatrix} + \frac{\partial}{\partial y} \begin{pmatrix} \rho v \\ 0 \\ h \end{pmatrix} = 0 \quad (4)$$

To enable boundary conditions to be conveniently imposed on a moving airfoil, the following coordinate transformation (illustrated schematically in Figure 1) is used:

$$X = x, Y = y - S(x,t), T = t, \quad (5)$$

where S accounts for both airfoil shape and motion.

$$\text{Transformed : } X = x, Y = y - S(x, t) \\ T = t$$



1232-016

Fig. 1 Sheared rectilinear computational grid about an airfoil.

Equation (4) is then transformed to

$$\frac{\partial}{\partial T} \begin{pmatrix} \rho \\ u \\ v \end{pmatrix} + \frac{\partial}{\partial X} \begin{pmatrix} \rho u \\ h \\ 0 \end{pmatrix} = \frac{\partial}{\partial Y} \begin{pmatrix} \rho(v - S_x u - S_t) \\ S_x h + S_t u \\ h - S_x v \end{pmatrix} = 0, \quad (6)$$

and, after some manipulation, is written

$$\frac{\partial}{\partial T} \begin{pmatrix} \rho \\ u + S_x v \\ v^x \end{pmatrix} + \frac{\partial}{\partial X} \begin{pmatrix} \rho u \\ h - S_x v \\ 0 \end{pmatrix} + \frac{\partial}{\partial Y} \begin{pmatrix} \rho(v - S_x u - S_t) \\ 0 \\ h - S_x v \end{pmatrix} = 0, \quad (7)$$

which also retains conservation form. Finally, the accompanying boundary condition of tangential flow can be written

$$v - S_x u - S_t = 0 \quad (8)$$

on $Y = 0$ from the leading to trailing edge of the airfoil.

For efficient computation, a coordinate stretching is employed in Y and X (ahead of and behind the airfoil), as illustrated in Figure 1. Various stretching are used in the sample calculations presented below. Two considerations are considered essential in every case: (1) The grid should be fine ($\Delta X, \Delta Y \approx 0.02$ chordlengths) in both directions near the airfoil and (2) the outer boundaries should be far enough away so that

signals cannot reflect off of them during the total time interval to be analyzed.

For lifting calculations, the Kutta condition is imposed along an un-deflected wake ($Y=0$) from the trailing edge to the far-field boundary by requiring density and normal-stream velocity be continuous across the wake.

At the far-field boundaries, the unperturbed flow is maintained.

NUMERICAL ALGOEITBMS

For simplicity in the following discussion, Equation (7) is denoted as

$$\frac{\partial W}{\partial T} + \frac{\partial F}{\partial X} + \frac{\partial G}{\partial Y} = 0 \quad (9)$$

where

$$W = \begin{pmatrix} \rho \\ u + S_x V \\ v \end{pmatrix}, \quad F = \begin{pmatrix} \rho u \\ h - S_x v \\ 0 \end{pmatrix}, \quad G = \begin{pmatrix} \rho(v - S_x u - S_y) \\ 0 \\ h - S_y v \end{pmatrix}$$

A predictor-corrector, explicit, differencing scheme has been constructed to assess the feasibility of the formulation. In this scheme, the new value W^{n+1} , at each time step is determined by an iteration consisting of a predictor step followed by several repetitions of a corrector step.

Define

$$\tilde{W}_{ij} \equiv W_{ij}^n - \frac{\Delta T}{2} (D_x F_{ij}^n + D_y G_{ij}^n + P_{ij}^n) \quad (10)$$

where P_{ij} denotes terms representing an artificial viscosity to be defined below. Then the predicted value is

$$W_{ij}^{n+1,1} = \tilde{W}_{ij} - \frac{\Delta T}{2} (D_x F_{ij}^n + D_y G_{ij}^n + P_{ij}^n) \quad (11)$$

The corrected value is formed by

$$W_{ij}^{n+1,k+1} = \tilde{W}_{ij} - \frac{\Delta T}{2} (D_x F_{ij}^{n,k} + D_y G_{ij}^{n,k} + P_{ij}^{n,k}) \quad (12)$$

An analysis of this scheme for a linear problem shows that it is unstable with one corrector step, but stable for a ΔT not greater than twice the Courant-Friedrichs-Levy condition¹⁶ when two corrector steps are used. The use of more than two correction steps is found to result in no further

Improvement. Numerical studies have confirmed these conclusions for the present non linear problem.

$$P_{ij} = \varepsilon (\Delta X D_x^+ (|u| + a) D_x^- + \Delta Y D_y^+ (|v| + a) D_y^-)_{ij} \quad (13)$$

where c is a positive number. Numerical studies have shown that a value of $\varepsilon = 0.25$ is sufficient to capture shocks and produce otherwise smooth pressures.

It should be noted that by using artificial viscosity no switching operator is required to capture the shock. This point is discussed in detail in Reference 15. As currently implemented, the artificial viscosity is used through out the flow field; however, experience with steady-state codes suggests that sharper shocks would result if the viscosity terms were eliminated in the subsonic regions.

For efficient flow calculations, an explicit scheme is far too slow. Consequently, after feasibility was demonstrated, an alternating-direction implicit differencing scheme was constructed, for which the selection of the time step is dependent only on the time scale of the motion being analyzed. This scheme is outlined

Let $\delta W_{ij} = W_{ij} - W_{ij}^n$. Then the Crank-Nicolson Scheme¹⁶ would be

$$\delta W_{ij} = -\frac{\Delta T}{2} (D_x F_{ij}^n + D_y G_{ij}^n) - \frac{\Delta T}{2} (D_x F_{ij}^{n+1} + D_y G_{ij}^n) \quad (15)$$

Approximating F^{n+1} and G^{n+1} by $F^n + A\delta W$ and $G^n + B\delta W$, where $A = \delta F/\delta W$ and $B = \delta G/\delta w$, this equation can be written as

$$\left(I + \frac{\Delta T}{2} (D_x A + D_y B) \right) \delta W_{ij} = -\Delta T (D_x F_{ij}^n + D_y G_{ij}^n) \quad (15)$$

and approximately factored as

$$\left(I + \frac{\Delta T}{2} D_x A \right) \left(I + \frac{\Delta T}{2} D_y B \right) \delta W_{ij} = -\Delta T (D_x F_{ij}^n + D_y G_{ij}^n) \quad (16)$$

W_{ij}^{n+1} can now be computed in two steps, each requiring the inversion of only a block tridiagonal matrix. Introducing artificial viscosity terms, the two steps are

$$\left(I + \frac{\Delta T}{2} (D_x A + \varepsilon \Delta X D_x^+ D_x^-) \right) \delta \tilde{W}_{ij} = -\Delta T (D_x F_{ij}^n + D_y G_{ij}^n + \varepsilon (\Delta X D_x^+ D_x^- + \Delta Y D_y^+ D_y^-) W_{ij}^n) \quad (17)$$

and

$$\left(I + \frac{\Delta T}{2} (D_y B + \varepsilon \Delta Y D_y^+ D_y^-) \right) \delta \tilde{W}_{ij} \quad (18)$$

To date, the scheme has been coded for the non-lifting case only.

SAMPLE RESULTS

Results obtained for various sample problems are discussed below together with comparisons with solutions generated by other methods. The grids used contained 3000 to 5000 points with a mesh width of approximately 0.02 chords near the airfoil. The computational times required depended, of course, on the mesh, the Courant number necessary for accuracy and the total time span of the particular problem. However, comparisons made with the low-frequency, small-perturbation code of Reference 10 (LTRAN) indicate that the present implicit scheme requires 13.5 times the computational work of LTRAN. This implies that a potential—function formulation based on the same techniques as the present primitive variable approach could be expected to require only 1.5 times the computation of LTRAN.

Thickening Airfoil

A problem that has been analyzed by several researchers is that of computing unsteady pressures on a bicircular arc airfoil which successively thickens and thins during its travel, as shown in Figure 2. The Mach number for this example is 0.85. The equation

$$TH = 0.1 \left[10 - 15 \left(\frac{30-r}{15} \right) + 6 \left(\frac{30-\tau}{15} \right)^2 \left(\frac{30-\tau}{15} \right)^3 \right],$$

$$15 \leq \tau \leq 30,$$

$$TH = 0, \quad \tau \geq 30 \quad (19)$$

where TH is the midchord thickness ratio and τ is time measured in c traveled. Consequently, the airfoil initially has zero thickness, grows to its maximum thickness of 10% after traveling 15 chordlengths and returns to zero thickness after traveling a total of 30 chord-lengths. During the

course of this travel, the variation of thickness causes an interesting flow-structure: A strong shock wave forms on the airfoil as it thickens; subsequently, as the air foil thins, the shock propagates rapidly up stream and leaves the airfoil nose to enter the oncoming flow. The numerical computation of this extensive shock motion is a rigorous test for unsteady transonic aerodynamic codes. It might be noted that because of their basic theoretical limitations, the methods of References 1-5 are unable to handle such cases of large shock motion.

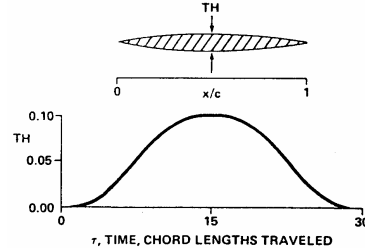


Fig. 2 Thickening-thinning airfoil motion.

Calculations by the present method will be compared with those of Reference 13 (full-potential equation in quasi-conservation form) and Reference 10 (small-perturbation, low-frequency equation in full-conservation form). The low-frequency approximation of the latter is considered valid for this case, though one might voice some concern during that portion of the time wherein the wave undergoes its rapid up stream motion. To facilitate the comparison, the computation grid used in the present calculations is patterned after that of Reference 10: In the stream-wise direction, the grid is uniform over the interval that extends from one chord-length upstream of the airfoil nose to the trailing edge; to either side of this interval, the grid is smoothly stretched to the boundaries located more than thirty chord-lengths from the airfoil. In the stream-normal direction, the grid is uniform from the airfoil surface to a distance of 0.2 chord-lengths; beyond this point the grid is stretched smoothing to a boundary also more than thirty chord-lengths from the airfoil. From studies of grid variation, it was concluded that the solution is sensitive to the choice of grids but that the present choice is adequate because it combines a fine-grid structure near the airfoil with boundaries sufficiently far removed for the present calculations. The grid used in Reference 13 is different from the above but that author states that sensitivity studies were performed to determine a sufficiently fine mesh.

Several solutions were generated with the present method using various time-step inter vals.

The algorithm was found to be stable at a Courant number, λ of as high as 40; but for solution accuracy $\lambda < 12$ (approximately) is required for this sample problem.

Results obtained by the three methods are shown in Figure 3a and 3b. In the first figure, the shock forms and strengthens. It should be mentioned that a significant lag occurs between the time the airfoil reaches maximum thickness ($\tau=15$) and the point ($\tau=18.25$) at which maximum shock strength is attained. In the second figure, the shock moves rapidly forward, while diminishing in strength, and leaves the airfoil. Although, as will be discussed in detail in the following paragraphs, there are some appreciable differences in the three solutions, the qualitative agreement between them is good.

Prior to and during the shock build-up, there are several discrepancies between the results of the three methods. At $\tau = 8.5$, both full-potential methods predict slightly less expansion over the forward part of the airfoil than does the small-perturbation method. At $\tau = 11.5$ and 18.25 , the shock positions and strengths computed by each method differ: The farthest aft and strongest shocks are predicted by the small-perturbation equation in conservation form; farthest forward and weakest shocks result from the full-potential equation in non-conservative form; and the shocks predicted by the present method (full-potential equation in fully conservative form) are intermediate in position and strength. This trend is consistent with well established steady-state transonic trends. The use of full-conservation form (FC) leads to shocks aft of those arising from non-conservation form (NC); the use of the small-perturbation equation leads to shocks aft of those arising from the full-potential equation. (See example comparisons in Reference 17.) It should be emphasized that the use of conservation form is essential to obtaining shock positions that are theoretically consistent with whichever aerodynamic formulation—small-perturbation or full-potential - is chosen for solution; consequently, the present method and that of Reference 10 are more correct in this aspect than the method of Reference 13. Finally, one can observe in Figure 3a that both full-potential methods predict a re-expansion after the shock at $\tau = 18.25$.

During the upstream motion of the shock, one notices that the shock speeds are somewhat different. In particular, the small-perturbation shock moves most rapidly and overtakes those of

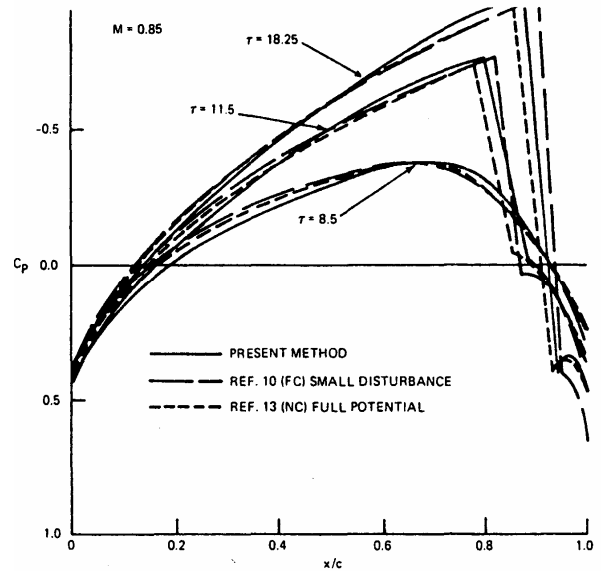


Fig. 3a Pressure coefficients on thickening-thinning bicircular-arc airfoil.

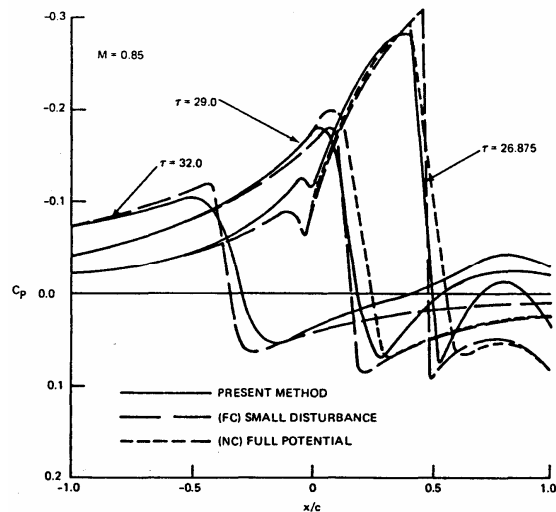


Fig. 3 b Pressure coefficients on thickening thinning bicircular airfoil

largest speed and overtakes that of Reference 13; and the shock of Reference 13 has the smallest Speed. This trend is consistent with the relative shock-strength maxima computed by the three methods. Finally, the present method is seen at the later times to predict a larger re-expansion behind the shock than do the other methods. The cause of this discrepancy is still under investigation.

a flap oscillating at a reduced frequency of 0.2 based on the airfoil chord. The flap, which deflects 5% has its leading edge and hinge line at the 75 percent chord. The plots start after several cycles have taken place and follow a half cycle in which the flap deflects downward, returns to the neutral position, and starts to deflect upward. At the first time slice, a lower-surface shock wave has formed at the hinge-line and an expansion is beginning to form on the upper surface.

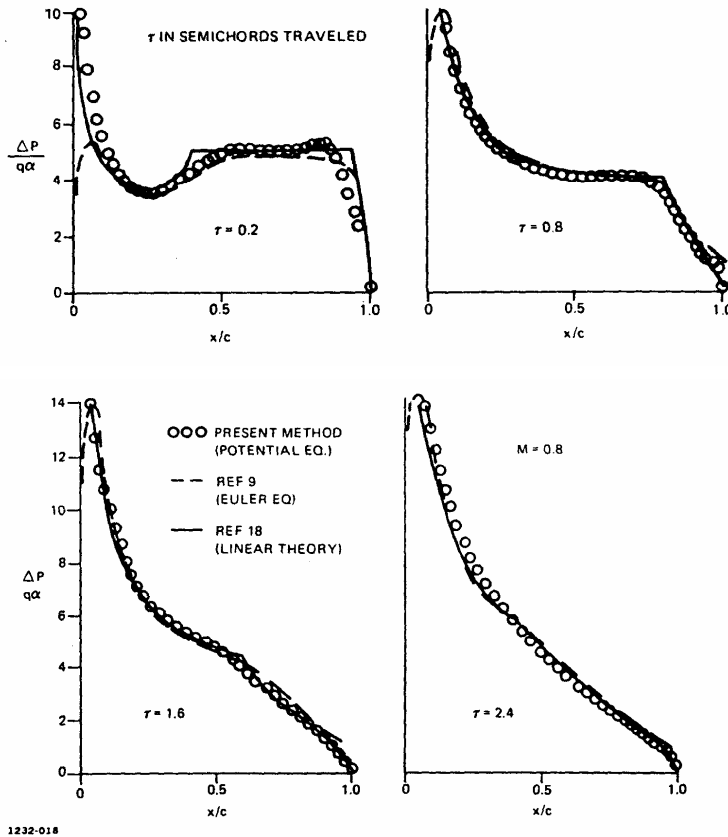


Fig. 4 Lifting pressures on a flat plate given an initial angle of attack of 1° at $\tau = 0$.

Flat Plate at Incidence

Results for a lifting case are presented in Figure 4. Lifting pressures are shown at various times on a flat plate at $M = 0.8$ given an initial angle of attack of 1° . Also shown are the solutions according to linear theory¹⁸ (roughly valid for this case) and Euler-equation solutions. Agreement between the three is excellent.

Oscillating Flap on a Bicircular-Arc Airfoil

Figure 5 Presents result surface pressures on a 10-percent-thick bicircular-arc-airfoil at $M = 0.8$ with

At the second time point, the shock has started moving forward, while the expansion has strengthened. This trend continues during the next time interval. By the fourth time slice, the shock can be seen to have weakened considerably during its upstream travel, while the expansion is beginning to weaken. At the fifth time slice (where the flap has returned to its neutral position). The shock and those at the first time point out with upper and lower-surface trends reversed.

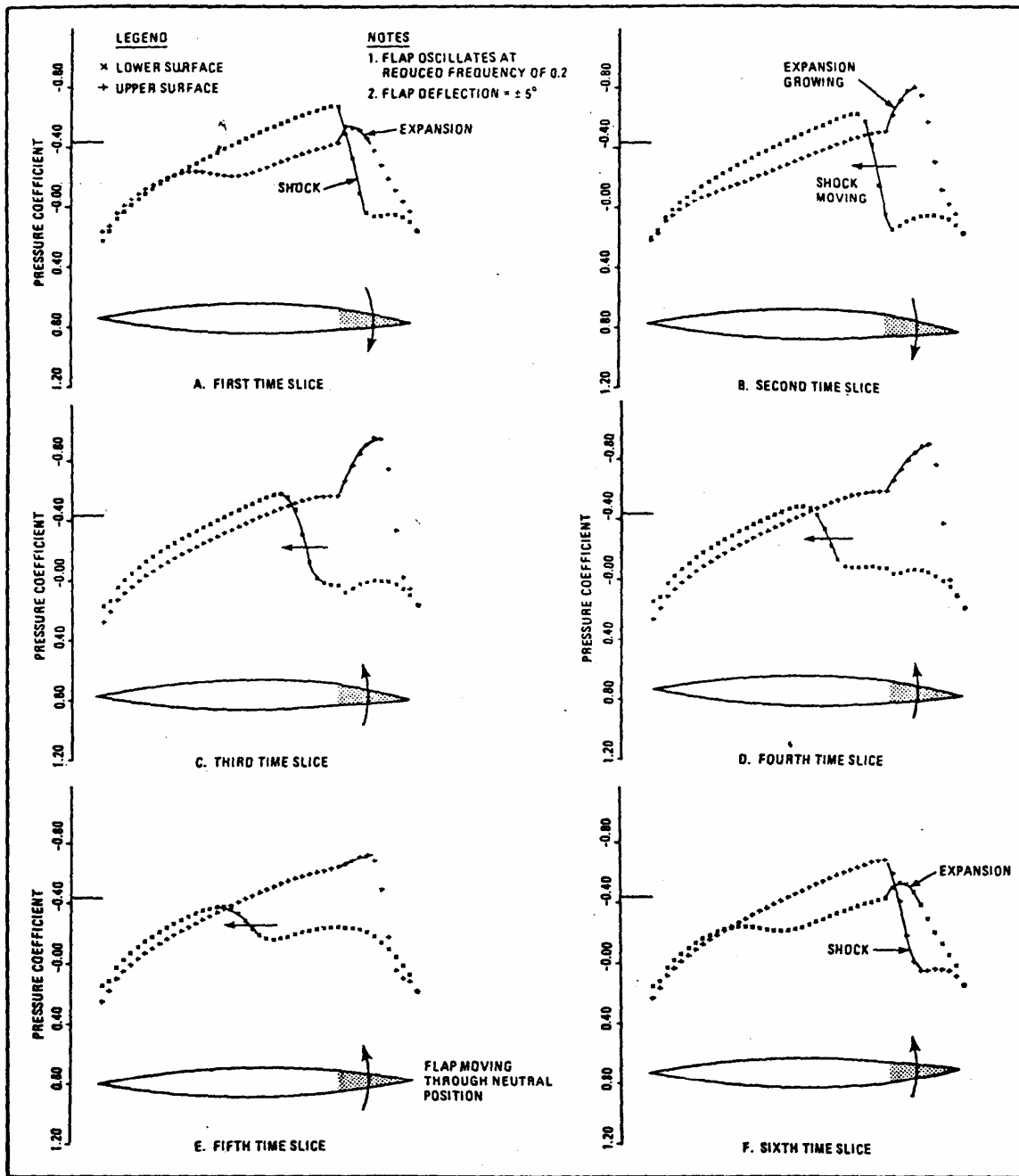


Fig. 5 Time History of the Surface Pressures on a 10% Thick, Bicircular-Arc Airfoil During a Cycle of Flap Oscillation ($M=0.8$)

NACA64A006 Airfoil

An additional test of an unsteady aerodynamics code is its ability to obtain a steady-state solution on a stationary airfoil. Calculations were run on an NACA646A006 airfoil at $M = 0.85$ with zero angle of attack placed into a uniform flow field at $\tau = 0$. The resulting pressure distribution after many chordlengths of travel have elapsed is shown in Figure 6 together with solutions from Reference 13 (full-potential equation in non-conservation form) and Reference 19 (Euler equations in conservation form). The present solution agrees better with the more-correct Euler-Equations solution than does that of Reference 13, particularly in regard to shock position and strength. Again, this is felt to be an indication of the necessity of a full-conservation-law formulation. The present method tends to smear the shock more than does Reference 19; but as stated above under "Numerical Algorithms," limiting the artificial viscosity terms to the supersonic regions would probably sharpen the shock. To obtain reasonable results for this blunt-nosed airfoil, it should be mentioned that the X-grid had to be chosen such that mesh points would straddle the nose. A curvilinear mapping about the nose would remove this requirement.

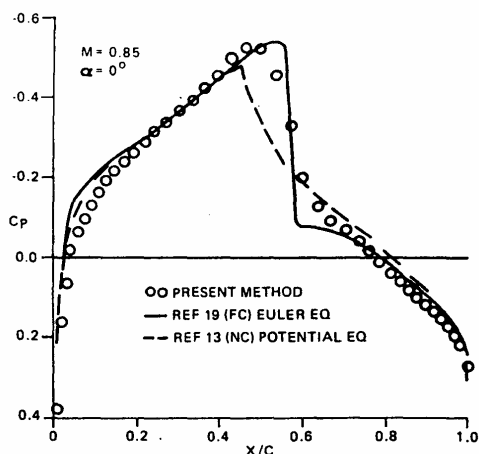


Fig. 6 Steady-state pressure Coefficients on NACA64A006.

CONCLUDING REMARKS

A method using primitive variables has been presented for obtaining accurate, efficient solutions to full-potential, unsteady, transonic flow about airfoils. The unique, key features of the approach are the retention of conservation be directly imposed on the airfoil surface, the inclusion of artificial-viscosity terms to capture shocks, and the construction of an implicit scheme (at least in the non-lifting case) for computational

efficiency. It is emphasized that the conservation form is necessary for the prediction of correct shock locations. Feasibility and accuracy of the approach have been demonstrated by several sample calculations, including ones wherein exceedingly large shock-wave excursions occur.

The work to date indicates the desirability of various modifications to the method. The restriction of artificial-viscosity terms to supersonic zones would reduce shock smearing. For more accurate treatment of blunt-nosed airfoils, curvilinear coordinate mappings should be introduced. To improve computational efficiency, the implicit algorithm should be extended to the lifting case. An alternating-direction-implicit algorithm can also be constructed along similar lines using a potential-function formulation, and further studies should be made to compare the accuracy and computational efficiency attainable with the present primitive-variable approach and such a potential-function formulation.

ACKNOWLEDGMENTS

The authors wish to express their appreciation to W. F. Ballhaus of the NASA Ames Research Center and P. Goorjian of Informatics Corporation for their critiques and suggestions.

REFERENCES

1. Ehlers, F. E., "A Finite Difference Method for the Solution of the Transonic Flow Around Harmonically Oscillating Wings," NASA CR-2257 July 1977.
2. Traci, R. M., Albano, E. D., and Farr, J. L., "Perturbation Method for Transonic Flows About Oscillating Airfoils," AIAA Journal, Vol. 14, No. 9, 1976.
3. Cunningham, A. M., "An Oscillatory Kernel Function Method for Lifting Surfaces in Mixed Transonic Flow," AIAA Paper No. 714 19714.
4. Liu, D. D., "A Lifting Surface Theory Based on an Unsteady Linearized Transonic Flow Model," AIAA Paper No. 78-501, 1978.
5. Fung, F. Y., Yu, N. J., and Seebass, B., "Small Unsteady Perturbations in Transonic Flows," AIAA Paper 77-675, 1977.
6. Tijdeman, H., "Investigations of the Transonic Flow Around Oscillating Airfoils," NLR Report TR 77090 U, 1978.
7. Magnus, B. J., and Yoshihara, H., "Unsteady Transonic Flow Over an Airfoil," AIAA Journal, Vol. 13, Dec. 1975.

8. Lerat, A., and Sides, J., "Calcul Numerique D'écoulements Transsoniques Instationnaires," ONERA TP No. 1977-19E.
9. "Transonic Flows with Circulation," NASA TN D—7605, 1975.
10. Ballhaus, W. F., and Steger, J. L., "Implicit Approximate-Factorization Schemes for the Low-Frequency Transonic Equation," NASA Th X-73,082, Nov. 1975.
11. Ballhaus, W. F., and Goorjian, P. N., "Implicit Finite Difference Computations of Unsteady Transonic Flows About Airfoils," AIAA Journal, Vol. 15, Dec. 1977.
12. Ballhaus, W. F., and Goorjian, P. M., "Computation of Unsteady Transonic Flows by the Indicial Method," AIAA Journal, Vol. 16, Feb. 1978.
13. Isogai, K., "Calculation of Unsteady Transonic Flow Over Oscillating Airfoils Using the Full Potential Equation," AIAA Paper 77—1977.
14. Goorjian, P. N., "Computations of Unsteady Transonic Flow Governed by the Conservative Full Potential Equation using an Alternating Direction Implicit Algorithm," NASA CR 152274 June 1979.
15. Notes of Lecture presented at the Von Karman Institute, Belgium, March 1976.
16. Isaacson, E., and Keller, H. B., Analysis of Numerical Methods Wiley and Sons, Inc., New York, 1966.
17. Ballhaus, W. F., "Some Recent Progress in Transonic Flow Computations," Notes of lecture presented at the Von Karman Institute, Belgium, March 1976.
18. Lomax, H., Heaslet, M. A., Fuller, F. B., and Sluder, L., "Two- and Three-Dimensional Unsteady Lift Problems in High Speed Flight," MACA Report 1077, 1952.
19. Magnus, R. J., "Calculations of Some Unsteady Transonic Flows about the MACA 6 and MACA 6 Airfoils," AYFDL—TB_77—146, July 1977.